AN INVESTIGATION OF THE RELATIONSHIP BETWEEN 'a'ā AND SPINY PĀHOEHOE AT THE HOLUHRAUN LAVA FIELD IN ICELAND

JONATHAN OTTO MAGEE, Franklin & Marshall College
Research Advisor: Andrew deWet

INTRODUCTION

The Holuhraun eruption occurred from 2014 to 2015 in response to caldera collapse at the Bárdarbunga volcano, which resides beneath the Vatnajökull ice cap. The area of collapse covered 110 square kilometers and descended 65 meters. A 48 km dike to Holuhraun withdrew magma from the 12 km reservoir, initiating the collapse (Gudmundsson et al., 2016). This field area was studied during the latter part of a month-long Keck Consortium project in Iceland looking at the Holuhraun and Laki volcanic fields. Within the Holuhraun volcanic field a distinctive change of morphology is seen at the end of the flow where spiny pāhoehoe lava or 'toothpaste' lava was observed to have discharge directly out of 'a'ā flows. This pattern was seen consistently across the volcanic flow in the aerial imagery studied. Multiple possible causes were investigated including geochemical changes, crystallization changes, changes in slope, changes in the cooling history, and changes in the effusion rates. The study combined field observations, remote sensing, whole rock and trace element geochemistry, petrographic observations and modeling to determine the cause of this change in morphology.

METHODS

In July 2016 during field study of the flow the two lava morphologies, 'a'ā and spiny pāhoehoe lava, were sampled at three locations along the northern edge of the flow. These locations were labeled as the vent-side margin (abbreviated VSM) – located near the vent at the beginning of the flow, the walk-in location (WIL) – located about half-way between the vent and the distal flow edge, and the hot springs (HS, featured
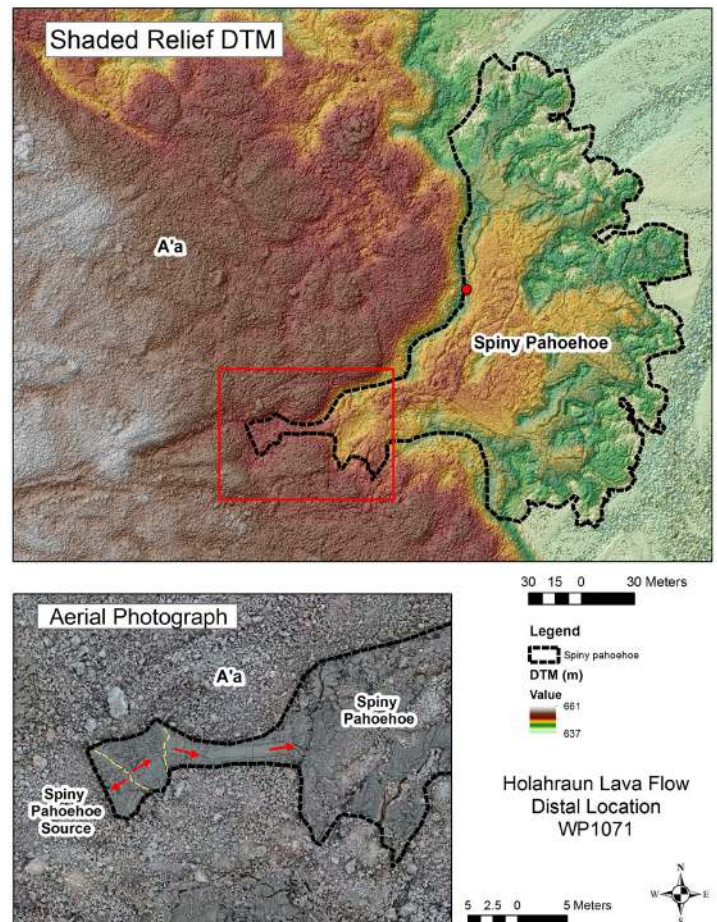

Figure 1. A shaded digital terrain map (DTM) and aerial drone photograph of the Hot Springs location illustrating the relationship between 'a'ā and spiny pāhoehoe. The spiny pāhoehoe breakout, illustrated with a dashed outline, is observed flowing out from the 'a'ā and through a small channel before expanding out onto the plain. Important to note is that the spiny pāhoehoe flow and its lobes are unbroken. If the 'a'ā was emplaced after these spiny flows then these would likely be partially covered due to the lower elevation.
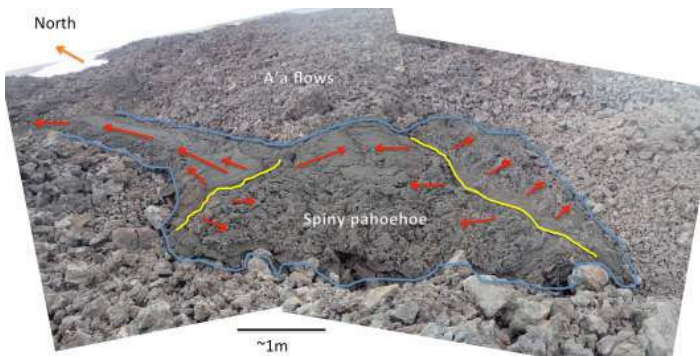
Figure 2. A ground-view of the outlined spiny pāhoehoe flow in Figure 1.

in Figure 1) – located at the extreme distal end of the flow. In addition to the basic spiny pāhoehoe and ʻaʻā lava types, additional samples were collected from the hot springs to characterize any possible homogeneities of the flow. This included inflated material as well as spiny pāhoehoe with a more slab-like form.

Once field work was completed all samples were sent by mail to Franklin and Marshall College for further analysis. Twenty-eight blanks were prepared and sent to Spectrum Petrographics to be made into thin sections. Eight samples were selected for geochemical analysis. The samples were prepared for XRF analysis,
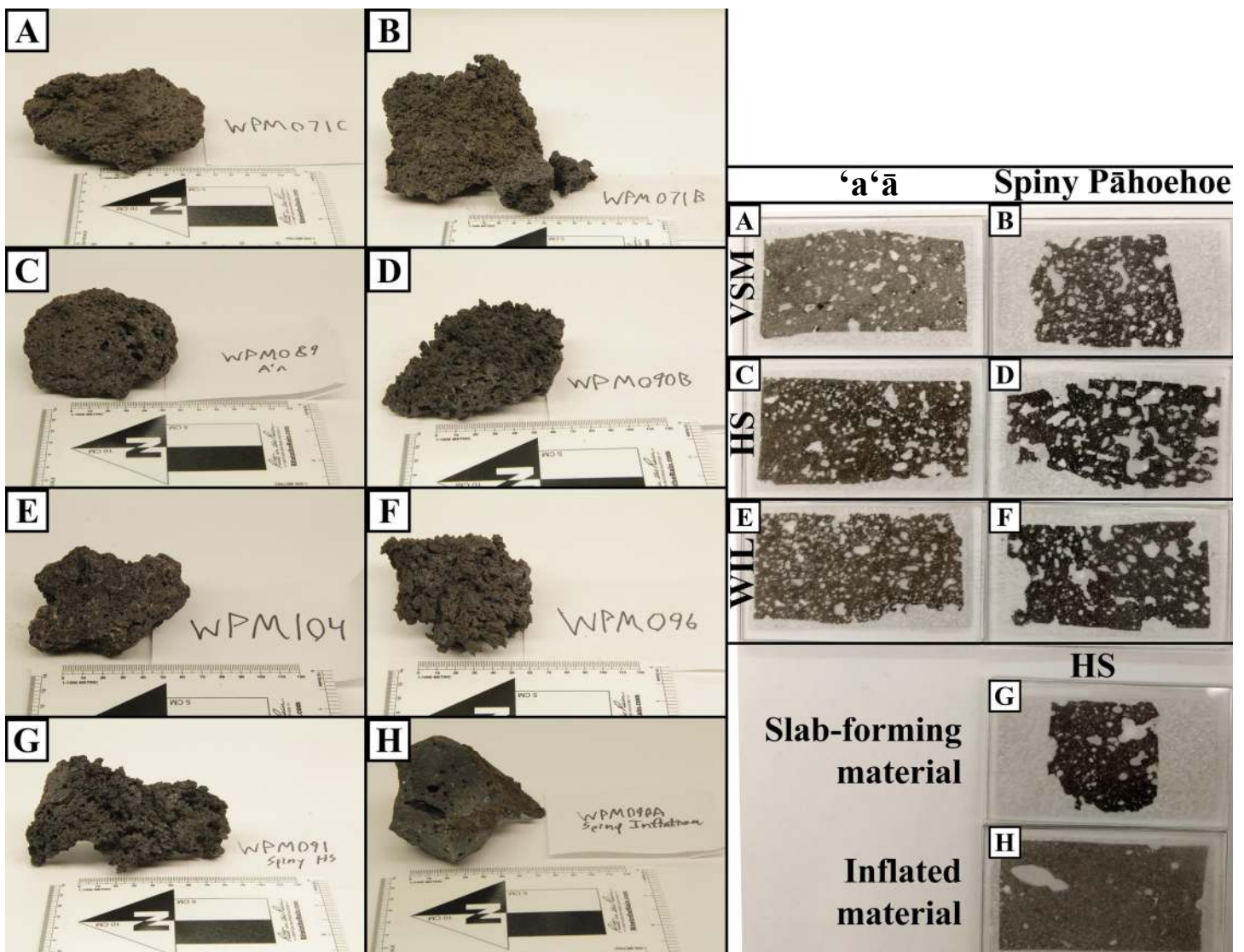

Figure 3. A) WPM071C, an ʻaʻā from the VSM and its corresponding thin section. B) WPM071B and thin section, from a spiny pāhoehoe at the VSM. C) WPM089 and thin section, a spiny pāhoehoe from the HS location. D) WPM090B and thin section, an ʻaʻā from the HS location. E) WPM104 and thin section, an ʻaʻā from the WIL. F) WPM096, a rubbly spiny pāhoehoe from the WIL. G) A piece of spiny and its thin section for the HS area. This sample was taken from a section that had a larger representation of spiny pāhoehoe slabs. H) A sample of inflated spiny pāhoehoe and its thin section from the HS. This piece was collected from an inflated section of the spiny pāhoehoe flow that had apparent magma wedging.

loss-on-ignition (LOI) and iron titration at F&M using standard procedures (https://www.fandm.edu/earth-environment/laboratory-facilities/xrf-and-xrd-lab, https://www.fandm.edu/earth-environment/laboratory-facilities/instrument-use-and-instructions/loi-and-iron-titrations-techniques). For each process specific samples were analyzed in duplicate or triplicate to assure the validity of the collected data. This information was then used to characterize the samples geochemically and generate CIPW normative analysis.

The thin sections were studied to characterize the differences between the different field morphologies and collect general information about the basalts. FOAMS (Shea et al., 2010), is currently being used to generate comparative data for vesicle analysis. Moving forward, density analysis would provide good information to compare to that generated by the FOAMS software. Further quantitative analysis of the thin sections would help to define modal differences, especially crystal size distributions.

The aerial photography and DTM data were collected using a Trimble UX5 unmanned automated vehicle (UAV) and processed by Stephen Scheidt at the University of Arizona.

RESULTS

Field & Sample Observations

The field area at Holuhraun provided excellent opportunities to observe the relationship between

Sample	Location	Morphology
WPM071B	VSM	Spiny Pāhoehoe
WPM071C	VSM	‘a‘ā
WPM089	HS	‘a‘ā
WPM090A	HS	Spiny Pāhoehoe
WPM090B	HS	Spiny Pāhoehoe
WPM091	HS	Spiny Pāhoehoe
WPM096	WIL	Spiny Pāhoehoe
WPM104	WIL	‘a‘ā

Table 1. A listing of the samples that were analyzed in this project, colour-coded by area and then morphology, where a darker fill colour represents ‘a‘ā of that area and a ligher fill colour represents spiny pāhoehoe.

‘a‘ā and spiny pāhoehoe. Study from the previous year assured that a relationship existed between these facies, but identifying structures within the field helped to dispel some uncertainties regarding it. The ‘a‘ā and spiny pāhoehoe are emplaced adjacent to each other, and the question at the beginning of this project was to identify the order of events that created this structure. In a volcanic field environment this could have been emplaced in two possible ways: either the ‘a‘ā flows are emplaced first and then spiny pāhoehoe flows from it, or the spiny pāhoehoe are emplaced first and then the ‘a‘ā flows were emplaced around and over the spiny pāhoehoe flows. Some features of these two flows seem to complicate the emplacement relationships, most notably the late inflation of the spiny pāhoehoe, which appeared to displace rubbly material during emplacement of the spiny pāhoehoe. In the scenario where ‘a‘ā flowed over the emplaced spiny pāhoehoe, one would expect the lava routing to diverge from existing forms and take the path of least resistance and cover parts of the spiny pāhoehoe flow. However, from field relationships such as rafted ‘a‘ā boulders and distinct mouth (Figure 2) and fountain locations it was determined that the spiny pāhoehoe must have flowed out of the ‘a‘ā flows. Additionally, the spiny pāhoehoe often filled between the lobes of the ‘a‘ā flows (Figure 1).

The ‘a‘ā and spiny pāhoehoe samples collected in the field have very distinctive characteristics (Figure 3). The spiny pāhoehoe samples collected are highly vesicular and jagged, except for the sample of inflated internal material (WPM090A). Vesicles in the spiny pāhoehoe are often joined together and elongate. The ‘a‘ā samples had fewer spiny surfaces and often the whole rock had an abraded surface texture. ‘a‘ā vesicles were smaller, more separate and more rounded. Marks and scratches from abrasion were much more apparent on the ‘a‘ā than on the spiny pāhoehoe.

Thin Section Analysis

A total of 14 thin sections were made from the rock samples at Holuhraun. Of these samples 8 were studied for this project. These samples are listed with morphology and location data in Table 1. Of the thin sections used in this study 3 are from ‘a‘ā samples and 5 are from spiny pāhoehoe. The extra spiny pāhoehoe
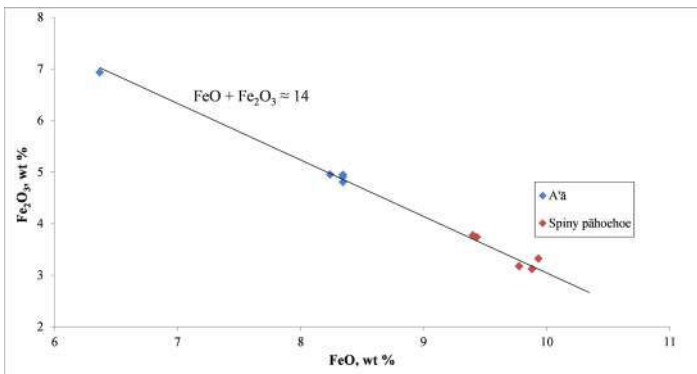
Figure 4. A graph relating Ferric and Ferrous iron in the sample. The average spiny pāhoehoe when compared to the average 'a'ā clearly has a deficiency in Fe2O3 (ferric iron) while being slightly enriched in FeO (ferrous iron). Though this difference can be seen in the preferred oxidation state, the total iron (represented here by the graph trendline) is very consistent. The total iron values as obtained XRF only varied by 0.11%. One of the 'a'ā samples (WPM104) had anomalous difference as compared to the average, it is not known why this is the case.
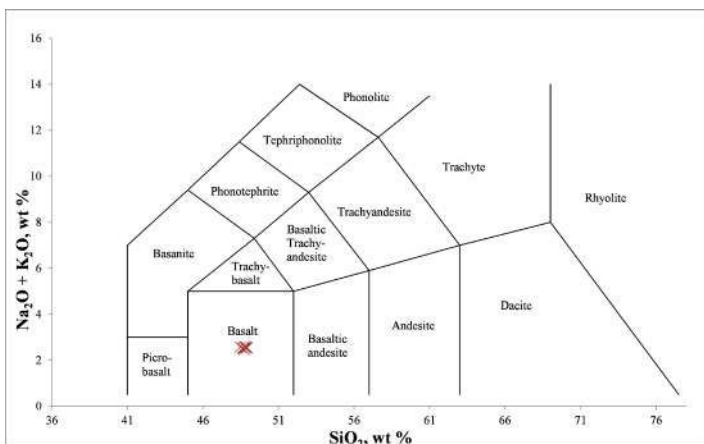

Figure 5. A TAS (total alkali-silica) diagram classifying all 8 samples as basalt. Though this implies homogeneity, observing other chemical signatures indicates that difference does exist between the two lava morphologies, notably the Fe2+/Fe3+ ratio highlighted in Figure 4.

samples come from the hot springs location and include one member that came from a slabby surface of spiny and one that was taken from the inflated side of the flow, where magma wedging was present.

Even without magnification, significant difference can be seen between the lava morphologies (Figure 2). The 'a'ā sections appear to be a darker shade of gray, and vesicles generally are seen to be less sheared and more rounded than in the spiny pāhoehoe thin sections. Under the microscope, the texture of all samples was

seen to be intergranular to intersertal. Plagioclase, olivine and clinopyroxene were the dominant anisotropic minerals. The gray colour was likely due to isotropic minerals such as magnetite, which can be seen more abundantly in the 'a'ā matrix.

Some small scale observations were made in thin-section that provide information about the crystallization history of the lava. In all samples clinopyroxene crystals were observed to have plagioclase trapped within them. The plagioclase often had a more pointed form, which likely indicates that these were encapsulated mid-crystallization. No clinopyroxene was observed within plagioclase, which indicates that of the two the plagioclase was likely first to crystallize. Sector zoning is seen in several clinopyroxene and plagioclase crystals, indicating a moderate speed of crystallization (Dowty, 1976). Alteration is visible most notably in the olivine observed. This secondary mineral is likely iddingsite, a common alteration product of olivine after surface emplacement (Gay and Le Maitre, 1961). Black, glassy vesicle rims are also common in the thin sections, these are amygdules, where gas precipitated to partially (or fully) fill in vesicle spaces(Morris, 1930).

X-ray Fluorescence, LOI, Iron Titration and CIPW Normative Analysis

The chemical make-up was very similar between samples (Figure 5), but clear differences were observed and could be correlated to the CIPW norm that was generated. The most apparent oxide difference is in the Fe_2O_3 and FeO. Where other oxide percentages vary by tenths of a percent, the average FeO concentration among the spiny pāhoehoe samples has 1.82% more FeO than the average A'ā, and has 1.92% less Fe_2O_3. This balances out quite well, as the total iron oxide percentages only differ by 0.11% between the averages, and this relationship is seen displayed in each sample's concentrations (Figure 4).

Trace element concentrations are also very similar between the samples, only the Sr, Y, Zr, Ni and Zn concentrations are seen to vary between the populations by more than a standard deviation. All of these element concentrations are greater in the spiny pāhoehoe, except for Ni.

FOAMS Vesicle Analysis

FOAMS was identified as an avenue for expediting vesicle analysis. The program would provide a uniform methodology with which the samples could be analyzed and only require the taking and editing of thin section photos. At present some issues have been encountered within the program, but once this is debugged this information will be quickly generated for the sample set.

DISCUSSION

Experimental differences and their interpretations

Experiments have been performed on the range of silicate liquids including basalt analyzing the Ferric-Ferrous iron ratio (Kilinc et al., 1983). Within this Sack *et al.* study the parameters controlling this relationship appear to be temperature, composition and oxygen fugacity. A study of similar Icelandic olivine tholeiites identified this ratio to correspond most closely to fugacity (öskarsson et al., 1994). The change in morphology as documented in the field is very abrupt, and if fugacity is the cause then the fugacity change is happening abruptly, rather than grading between the two members. This theory supports a vent-driven change, as local change would likely have a visible gradient connecting the two morphologies, occurring during the time-scale of the eruption.

Small chemical differences were observed between the two sample sets in the trace element concentrations. The most notable differences were those of Sr, Y, Zr, Ni and Zn. A possibility is that this difference is just a product of fractionation due to cooling. Sr, Y and Zn are notably incompatible elements, while Ni is very compatible (Winter, 2001). In composition to the 'a'ā the spiny pāhoehoe was relatively enriched in Sr, Y and Zn, while being depleted in Ni. While this is a broad transition, it is also the end of the lava flow and the final crystallization of melt, and such elemental differences could be notable in comparison to material that crystallized early on.

These chemical differences are what influence the differences in the calculated CIPW norms, and variation in the Ferric-Ferrous iron ratio appeared to have the largest impact. Hypersthene, (Mg, Fe^{2+})$_2$Si$_2$O$_6$, and magnetite, Fe^{2+}Fe^{3+}$_2$O$_4$, had the largest variation between morphologies. A higher concentration of magnetite is predicted in the 'a'ā norms than the spiny pāhoehoe, and a higher concentration of hypersthene is predicted in the spiny pāhoehoe than the 'a'ā norms.

Because the ratio of Ferric to Ferrous iron in magnetite's chemical formula is 2:1, it would be expected that the closer the actual chemical concentrations match this ratio, the more magnetite would be produced. The calculated ratios match this trend exactly as expected. While spiny pāhoehoe generally has a ratio around 0.3, the ratio in the 'a'ā samples averages to 0.65, and the one anomalous 'a'ā has a ratio of 0.98.

Magma evolution

The chemical data has shown that all samples would be classified as basalts, yet this classification can be narrowed down further to provide ideas for the history of this flow. Based on thin section analysis and chemical data it is very likely that the lava is evolved and well-fractionated. Ni and Cr are both elements that indicate fresh, unfractionated lava, but in the samples these concentrations are low, less than 100 ppm in all cases. Additionally, even though olivine is present in all samples, very little spinel was found, which indicates that the source melt has remained near the surface for a while before the eruption (Winter, 2001).

CONCLUSIONS

Current Hypotheses

A large amount of data has been generated and reviewed in the process of this study. This effort has aimed to identify what differences may cause the flow transition observed in the field at Holuhraun. No single answer has been found currently, but small leads exist and more will likely appear as further research is completed. Some change did alter the chemistry of the flow, causing a discrepancy in the ferric-ferrous iron ratio between the two morphologies. Oxygen fugacity has arisen as a possible cause for chemical change, and perhaps for the entire morphological change. If this is the case then the surface changes are likely due to slow evolution and changes in the source caldera or

the dike feeding the eruption, as partial pressures of oxygen shouldn't change so quickly,

Further Research

Further study of the two lava morphologies and their interactions will look into some new details while reflecting on what is currently known. A method for determining sample densities is included in Shea et al (2009), and will be good to compare with estimates of density made by the FOAMS program to assess accuracy of the software for the samples in this project. The thin sections have been reviewed thus far, but further work could be done on them to quantify modal differences between the two samples.

ACKNOWLEDGEMENTS

REFERENCES

Dowty, E., 1976, Crystal structure and crystal growth: II. Sector zoning in minerals : American Mineralogist, v. 61, p. 460.

Gay, P., and Le Maitre, R.W., 1961, Some Observations on Iddingsite: American Mineralogist, v. 46, p. 92–111.

Gudmundsson, A., 2000, DYNAMICS OF VOLCANIC SYSTEMS IN ICELAND: Example of Tectonism and Volcanism at Juxtaposed Hot Spot and Mid-Ocean Ridge Systems: Annu. Rev. Earth Planet. Sci, v. 28, p. 107–40, doi: 10.1146/ annurev-earth-28-042010-200001.

Gudmundsson, M.T., Jónsdóttir, K., Hooper, A., Holohan, E.P., Halldórsson, S.A., Ófeigsson, B.G., Cesca, S., Vogfjörd, K.S., Sigmundsson, F., Högnadóttir, T., Einarsson, P., Sigmarsson, O., Jarosch, A.H., Jónasson, K., et al., 2016, Gradual caldera collapse at Bárdarbunga volcano, Iceland, regulated by lateral magma outflow: Science, v. 353, no. 6296, p. 1–24, doi: 10.1126/science. aaf8988.sciencemag.org.

Kilinc, A., Carmichael, I.S.E., Rivers, M.L., and Sack, R.O., 1983, The ferric-ferrous ratio of natural silicate liquids equilibrated in air: Contributions to Mineralogy and Petrology, v. 83, no. 1–2, p. 136–140, doi: 10.1007/BF00373086.

Morris, F.K., 1930, Amygdules and pseudo-amygdules: Geological Society of America Bulletin, v. 41, no. 3, p. 383–404.

öskarsson, N., Helgason, o., and Steinthórsson, S., 1994, Oxidation state of iron in mantle-derived magmas of the Icelandic rift zone: Hyperfine Interactions, v. 91, no. 1, p. 733–737, doi: 10.1007/BF02064599.

Shea, T., Houghton, B.F., Gurioli, L., Cashman, K. V., Hammer, J.E., and Hobden, B.J., 2010, Textural studies of vesicles in volcanic rocks: An integrated methodology: Journal of Volcanology and Geothermal Research, v. 190, no. 3–4, p. 271–289, doi: 10.1016/j.jvolgeores.2009.12.003.

Winter, J.D., 2001, An Introduction to Igneous and Metamorphic Petrology: